

# Diffusion Tensor Tractography Visualizes Partial Nerve Laceration Severity as Early as 1 Week After Surgical Repair in a Rat Model Ex Vivo

Angel F. Farinas, MD\*; Isaac V. Manzanera Esteve, PhD†§; Alonda C. Pollins, MLI\*; Nancy L. Cardwell, BS\*; Mark D. Does, PhD†‡§; Richard D. Dortch, PhD†‡§; Wesley P. Thayer, MD, PhD\*†

**ABSTRACT** Background: Previous studies in our laboratory have demonstrated that a magnetic resonance imaging method called diffusion tensor imaging (DTI) can differentiate between crush and complete transection peripheral nerve injuries in a rat model ex vivo. DTI measures the directionally dependent effect of tissue barriers on the random diffusion of water molecules. In ordered tissues such as nerves, this information can be used to reconstruct the primary direction of diffusion along fiber tracts, which may provide information on fiber tract continuity after nerve injury and surgical repair. Methods: Sprague-Dawley rats were treated with different degrees of partial transection of the sciatic nerve followed by immediate repair and euthanized after 1 week of recovery. Nerves were then harvested, fixed, and scanned with a 7 Tesla magnetic resonance imaging to obtain DTI and fiber tractography in each sample. Additional behavioral (sciatic function index, foot fault asymmetry) and histological (Toluidine blue staining) assessments were performed for validation. Results: Tractography yielded a visual representation of the degree of injury that correlated with behavioral and histological evaluations. Conclusions: DTI tractography is a noninvasive tool that can yield a visual representation of a partial nerve transection as early as 1 week after surgical repair.

## INTRODUCTION

During the period from World War II to the Global War Against Terrorism, mortality has decreased from 30 to 10% because of improved protective technology and more effective field evacuations.<sup>1</sup> Current procedures to preserve life, as well as limb, are applied immediately at the battlefield, helping to delay definitive treatment that could be miles away.<sup>2</sup> Improving combat survival has subsequently increased the number of complex wounds in which peripheral nerve morbidity is high.<sup>3</sup> In Operation Iraqi Freedom and Operation Enduring Freedom only, more than half of the injuries involved extremities.<sup>4</sup> Injuries to the extremities is the most common cause of disability after a combat wound, and disability involving peripheral nerve injuries can be as high as 70%.<sup>5</sup> Some authors

have described that approximately 70% of the traumatic nerve injuries were caused by an explosion.<sup>3,5</sup> In the upper extremity, the radial nerve is the most common culprit of disability in a wounded soldier, but the ulnar nerve at the level of the forearm is most common nerve injured.<sup>3,5</sup> Disability can be defined as loss of function, military discharge, or chronic pain.<sup>3</sup>

According to Seddon, nerve injury can be classified depending on the degree of injury<sup>6</sup> including compression with or without demyelination (neurapraxia), axon transection with remaining layers intact (axonotmesis), and complete transection (neurotmesis).<sup>6</sup> Sunderland revised this classification into five degrees. The first- and second-degree injuries correlated with neurapraxia and axonotmesis, respectively. Sunderland also included two more degrees of injury dependent on if the endoneurium (third degree) or perineurium (fourth degree) was involved. Finally, fifth degree represent complete transection when all layers are injured, which is equivalent to Seddon's neurotmesis.<sup>6</sup> In a study done by Birch et al.,<sup>3</sup> where a total of 261 peripheral nerve injuries caused in Iraq and Afghanistan's warfare were observed, 45% were neurapraxia, 35% were axonotmesis, and 20% were neurotmesis, distributed equally between the upper and lower extremities.

The vast majority of experience with peripheral nerve repair comes from the military arena, mainly because of the caliber of the weapons involved in these injuries.<sup>5</sup> The incidence of traumatic peripheral nerve injuries after Iraq's and Afghanistan's conflicts was 8%.<sup>3</sup> But peripheral injuries are not exclusive of wartime; this morbidity is also encountered in the civilian hospitals as well. Each year, approximately 800,000 patients seen in trauma centers with some sort of peripheral nerve injury.<sup>7</sup>

\*Department of Plastic Surgery, Vanderbilt University Medical Center, 1161 21st Ave S, MCN D4207, Nashville, TN 37232-2345

†Department of Biomedical Engineering, Vanderbilt University, 2301 Vanderbilt Place PMB 351631, Nashville, TN 37235-1631

‡Department Radiology and Radiological Sciences, Vanderbilt University Medical Center, 1161 21st Ave S, MCN CC-1121, Nashville, TN 37232-2345

§The Department is the Vanderbilt University Institute of Imaging Science, Vanderbilt University Medical Center, Vanderbilt University, Institute of Imaging Science, 1161 21st Ave S, MCN AA-1105, Nashville, TN 37232-2345

Presented as oral talk at the 2018 Military Health Science and Research Symposium August 20–24, Kissimmee, FL; Abstract Number: MHSRS-18-1268.

This work was supported by U.S. Army Medical Research and Materiel Command, Contract Number W81XWH-15-JPC-8/CRMRP-NMSIRA, Grant number: MR150075. Additional support provided by NIH/NINDS R01 NS97821 (RDD).

doi:10.1093/milmed/usz360

© Association of Military Surgeons of the United States 2020. All rights reserved. For permissions, please e-mail: journals.permissions@oup.com

Management of a peripheral nerve injury differs from the community to the combat zone. In the civilian setting, depending on the nature of the injury and concomitant injuries, these can be repaired immediately or delayed.<sup>8</sup> Immediate repair after injury has surgical advantages including avoiding edema and scar tissue. Additionally, the topographic alignment with intraoperative stimulation can be useful in complex wounds.<sup>8</sup> Conversely, in war periods, when a soldier suffers a peripheral nerve injury, they undergo damage control, serial debridement/decontamination, temporary bone stabilization, and plan for final repair and soft tissue coverage on a posterior date.<sup>2</sup> All combat wounds are considered contaminated with a high incidence of osteomyelitis if closed by primary intention.<sup>3</sup> Nerve repair is mostly achieved in a delayed fashion because of the heavily contaminated wounds.<sup>2</sup> Segmental nerve loss typically treated with an autograft can be troublesome because of limited sources of donor tissue secondary to polytrauma and limb amputations.<sup>2</sup> At the time of formal neurotomy, it is recommended to perform a nerve transfer because of the uncertain patient follow-up.<sup>2</sup>

Currently, clinical evaluation and electrodiagnostic tests are the only two ways to evaluate nerve outgrowth after repair. Clinical evaluation is a waiting game because it is subject to the rule of axonal growth at a speed of 1 mm/day, and subsequent reinnervation of the muscle.<sup>8</sup> The relevant information about regeneration will be delayed until the axons reach the end plate. Tinel sign is an important component of sensory level evaluation, which in some patients could be an unpleasant experience, especially if they have neuromas or post-injury pain sequela.<sup>3,9</sup> Another option, performing an electromyography, also has the disadvantage of being painful because of its invasive nature to access the target muscle. Electromyography is also time sensitive because it cannot be performed before 3 weeks post-injury when denervated fibrillations appear.<sup>9,10</sup> After repair, axonal regeneration is monitored every 90 days.<sup>9</sup> But, unless the axonal outgrowth reinnervates the end plate, no relevant information can be obtained about the status of the repair. Unfortunately, this forces us, as health care providers, to adapt a “watch and wait” approach to assess nerve recovery. In some cases, the interval surpasses our expectation allowing irreversible muscular atrophy to set in. Developing a prompt, noninvasive, and accurate tool for nerve outgrowth, assessment has been the focus of our team for the past years.

Diffusion tensor imaging (DTI) is a magnetic resonance imaging (MRI) method that measures the effect of tissue barriers on the diffusion of water molecules behavior at a microstructural level. In ordered tissues such as nerves, the effect of tissue barriers is larger perpendicular to the axons than parallel to them, resulting in diffusion anisotropy; changes in anisotropy have been correlated with pathological changes following nerve damage and recovery.<sup>11,12</sup> From DTI, one can estimate a number of scalar indices, including the axial, radial, and mean diffusivities (AD/RD/MD) as well as the fractional anisotropy (FA = 0–1, with higher

values representing higher anisotropy). Axial diffusivities represents the fastest diffusion direction along the axis of the nerve. Radial diffusivities represents slower diffusion in the transverse axis of the nerve, which is modulated by myelin and axonal densities.<sup>13</sup> Mean diffusivities is the average diffusivity across all directions, which is equivalent to the mean apparent diffusion coefficient.<sup>12</sup> In addition to these scalar indices, diffusion tensor tractography (DTT), which reconstructs fiber tracts based upon the estimated fast diffusion direction in neighboring voxels, can be performed from DTI data.

Scalar DTI indices provide little information within the first 4 weeks of Wallerian degeneration because of the effect of edema. Here, we develop a DTT that included additional orientation information to assess early nerve regeneration 1 week after partial transection and surgical repair. Additional behavioral assessments (sciatic function index [SFI], foot fault [FF] asymmetry) and histology (Toluidine blue staining) were performed for validation purposes.

## METHODS

### Animals

After obtaining Institutional Animal Care and Use Committee approval (application number M16000-99), as well as Animal Care and Use Review Office approval, female Sprague-Dawley rats between 8 and 12 weeks of age were randomly divided into groups of six animals. The groups included 25, 50, or 75% partial nerve transection as well as sham. All animals were housed in our central animal care facility where they had access to food and water ad libitum with 12 hours light/dark cycle and in accordance with the Guide for Care and Use of Laboratory Animals to minimize pain and suffering.

### Surgery

Under general anesthesia with isoflurane 2% at a dose of 3 mL/min, the surgical area was clipped, then prepped with chlorhexidine and draped. All the procedures were performed on the left hind limb. A 3-cm longitudinal incision was performed from the ischial notch down, parallel to the femur's longer axis. Using a split muscle technique, the sciatic nerve was identified and dissected free from the surrounding tissue. The sham group consisted of freeing up the nerve, no intervention and closure. The partial transection injury was created with number 15 stainless steel blade, and the partial injury device shown in [Supplemental Figure 1](#) was placed at least 1 cm proximal to the trifurcation of the nerve. The devices were custom manufactured with varying groove depths to create 25, 50, or 75% injuries using a Monoprice Maker Ultimate 3D Printer, Monoprice, Inc, Rancho Cucamonga, CA and consisted of 100% polylactic acid plastic. Devices were sterilized via ethylene oxide before use in surgery. After transection, the injury was repaired immediately using interrupted epineurial 9-0 nylon sutures (Ethicon, Somerville, NJ) under an operating microscope.

All wounds were irrigated profusely with Ringer's lactated solution and closed in layers using 5-0 Monocryl suture (Ethicon, Somerville, NJ). The animals were monitored in recovery and transported back in stable conditions to our animal facility. All animals received meloxicam (2 mg/kg) subcutaneously daily for 3 days post-procedure for analgesia.

### Nerve Samples

Once reaching the first post-operative week, each rat was euthanized under heavy anesthesia with euthasol (Virbac AH, Fort Worth, Texas) at 120 mg/kg placed intracardiac and sciatic nerves were harvested. Harvested nerves were fixed in 2% paraformaldehyde/3% glutaraldehyde in phosphate buffer solution for 24 hours and then washed for 7 (7) days in phosphate buffered solution to remove excess fixative and doped with 1 mM gadolinium diethylene triamine pentaacetic acid (Magnevist, Bayer healthCare, Bayer Healthcare Pharmaceuticals, LLC, Berlin, Germany) to reduce MRI relaxation and scan times.

### Behavioral Testing

Clinical evaluations consist of two components: SFI and FF. Our assessments were performed pre-operatively, post-operative day 3 and day 7, and immediately before euthanasia. To obtain SFI, rats were trained to climb a beam, and, after performing without hesitation, each hind paw was inked with different colors and recorded on a paper strip applied to the wooden beam. Three consecutive foot prints with each limb were recorded and measured. The operated limb was considered the experimental, and the contralateral one was identified as normal. Each print was examined, and function was quantified with the following: normal print length (NPL), normal toe spread (NTS), normal intermediary toe spread (NIT), experimental print length, experimental toe spread, and experimental intermediary toe spread. Sciatic Functional Index scores were calculated using the formula:  $SFI = -38.3([\text{experimental print length} - \text{NPL}]/\text{NPL}) + 109.5([\text{experimental toe spread} - \text{NTS}]/\text{NTS}) + 13.3([\text{experimental intermediary toe spread} - \text{NIT}]/\text{NIT}) - 8.8$ .<sup>14</sup> To obtain FF data, each rat was placed in a grid with 2.5 cm<sup>2</sup> apertures raised 2 cm from the base, and a total of 50 forward steps with each hind limb was recorded. A full fault was recorded when the posterior foot touched the floor, although a partial fault was recorded when the foot passed through the grid but did not touch the underlying floor. The FF score was calculated using the formula: composite FF score = (*n* partial faults × 1) + (*n* full faults × 2), %FF = (composite FF score/total number of steps) 100%, FF asymmetry score = %FF (normal hind limb) – %FF (surgical hind limb).<sup>14</sup>

### Imaging

MRI was performed *ex vivo* using a 7-T, 16-cm bore Varian Direct Drive scanner and 25-mm quadrature Doty Scientific. DTI data were collected using a 3D pulsed

gradient spin-echo sequence with 20 diffusion directions and  $b = 2,000 \text{ s/mm}^2$  ( $\delta/\Delta = 4/12 \text{ ms}$ ). Additional parameters included: FOV =  $6 \times 6 \times 16 \text{ mm}^3$ , NEX (number of excitations) = 2, TE/TR = 22/425 ms, resolution =  $125 \times 125 \times 372 \mu\text{m}^3$  and a scan time = 7 hours, 40 minutes. Diffusion tensors scalar metrics (FA, AD/RD/MD) and diffusion directions (visualized via diffusion ellipsoids) were estimated using in-house written code (MATLAB).<sup>15</sup> Fiber tracking was additionally performed for visualization purposes using the MATLAB toolbox ExploreDTI. Quantification of cut depth in a nerve was obtained by measuring the number of pixels within the nerve, whose correspondent diffusion ellipsoid's major axis was oriented in the *x-y* axis (i.e., not in the primary direction of the nerve fibers, which were oriented along the *z*-axis) and divided by the total number of pixels in the corresponding slice. These measurements were performed in each slice of the proximal transected and distal region of the nerve providing the percentage of the cut depth. Voxels at the boundaries of the nerve tissue were excluded from this analysis to minimize the impact of partial volume averaging with surrounding tissue.

### Histology

Following MRI scanning, harvested nerves were post-fixed with 1% OsO<sub>4</sub> solution, dehydrated through increasing concentrations of ethanol, and then embedded in resin at 60° for 72 hours. Embedded specimens were sectioned at 1- $\mu\text{m}$  and stained with 1% toluidine blue. Digital images of sections were acquired on an Olympus C-35 AD-4 microscope. The entire cross-section was imaged at 20X, and additional random 40X images (3 each) were captured from representative healthy and injured regions. Using Image-Pro plus 7.0 software, healthy and injured area measurements were quantified from 20X images. Axons within each 40X image were counted manually using the count tool in Photoshop CS5 Extended Edition, and density (number/mm<sup>2</sup>) measurements were calculated for healthy and injured areas. Total axon counts were calculated by multiplying axon density by healthy and injured areas calculated from 20X images and then summing the average total axons for the two regions. Percent injury was calculated by comparing total axon measurements made distal to the injury site against total axon measurements proximal to the injury site, with each nerve serving as its own control. Percent injury was averaged for each experimental group.

### Statistics

A single factor analysis of variance was performed to test for significant variations across all groups followed by post-hoc pairwise *t*-tests across each group. After Bonferroni correction, statistical significance was deemed for *p*-values < 0.05.

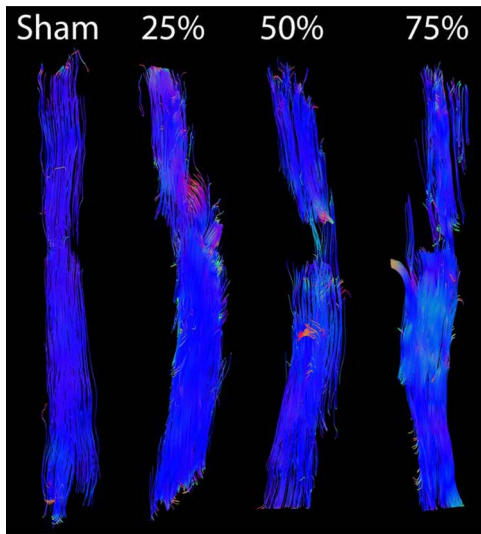


**FIGURE 1.** DTT of the sham and partially injured rat sciatic nerve. Notice that the sham image has full tracts without interruption. The degree of interruption increases as the partial injury increased.

**RESULTS**

Fiber tracts for sham and several degrees of partial cuts (25, 50, and 75%) are shown in Figure 1. DTT in sham nerves indicate that all fibers remained intact throughout the length of the nerve. Partially injured nerves show the severity in the discontinuity of fiber tracks in the transected region. Depending on the depth of the injury, the interruption is bigger or smaller in the tractography images. Ellipsoidal maps in a sagittal plane, shown in Supplemental Figure 2, display noninjured regions as blue ellipsoids whose semimajor axis is oriented in the z-direction. Meanwhile, red and green ellipsoids represent orientation in x- and y-directions, indicating disruptions of fiber coherence. In Supplemental Figure 2, the center image shows ellipsoidal maps from multiple axial locations along the nerve, although the right-hand side of the image displays more detailed ellipsoidal maps from the proximal, transected, and distal regions. It is clear that fiber orientation disruption only happens at the transected region, while fibers are more organized in the healthy areas proximal and distal to the injury. When analyzing the ellipsoid’s major axis orientations and the fiber disruption at the site injury, Figure 2 illustrates the directionality of the fibers for nerves as grouped by injury depth. Mean values are calculated and represented by black lines. Quantitative assessment of cut severity in Figure 2 indicates that the proposed method can be assay damage severity 1 week after injury/repair.

Upon clinical evaluations of these animals, we see that FF values in all groups decrease on postoperative day 3 consistently compared with baseline (Supplemental Figure 3A). However, the 25% group recovers to almost preoperative values within 1 week. The remaining two groups have a proportional decrease with expected recovery at week 1, in which the 50% cohort was lower than the 25% cohort, but

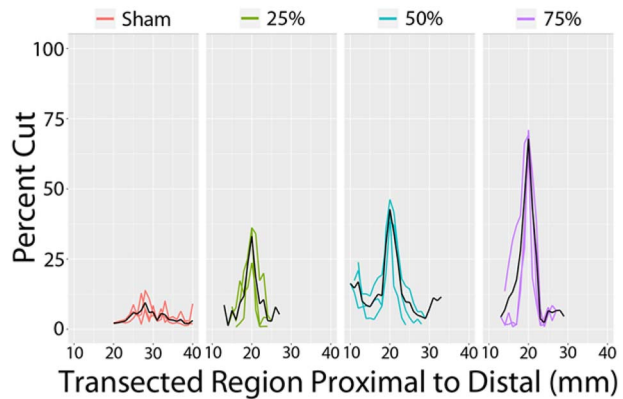


**FIGURE 2.** Quantitative measurements of transected nerves severity. Sham nerves (0% injury) is used as base line for cut depths of 25, 50, and 75%. Means ( $n = 3$ ) are represented by the black lines.

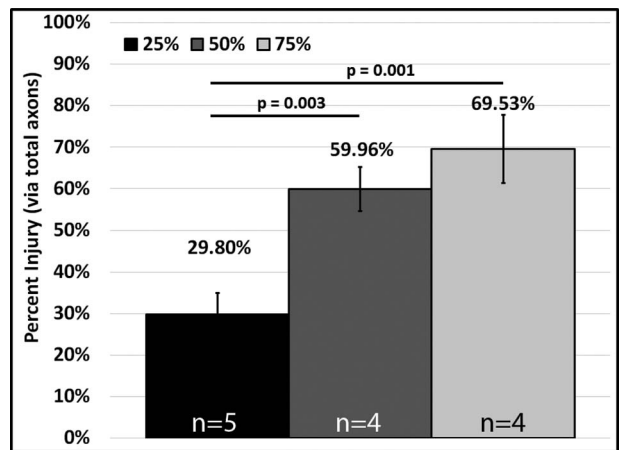


**FIGURE 3.** Axon counting of the injury area compared with total cross-section of the nerve. Statistical significant difference between 25% group versus 50% group ( $p < 0.05$ ) and 25% group versus 75% group ( $p < 0.005$ ).

higher than the 75% cohort. Regarding SFI, all groups had expected decreased scores on the earliest post-operative evaluation, but recovery was much slower than FF at 1 week (Supplemental Figure 3B). There was virtually no difference between post-operative day 3 values and those at 1 week, except for in the 75% injured, which improved slightly, though still did not approach baseline. Histology methods were also deployed for data for validation, and total axons were calculated from cross-sectional areas proximal and distal to the injury and repair (Fig. 3). The mean area of injury calculated for the 25% group was 29.80% ( $\pm 5.21\%$ ). For the 50% group, the injured area calculated was 59.96% ( $\pm 5.33\%$ ) with statistical significance compared with the former group ( $p < 0.005$ ). Concerning the 75% group, the injured area calculated was 69.53% ( $\pm 6.86\%$ ), also with statistical significance compared with the 25% group ( $p < 0.005$ ).

## DISCUSSION

Soldiers injured in action who suffer a peripheral nerve damage are frequently injured by improvised explosive devices.<sup>16</sup> Explosion injuries in periods of conflict have been strongly associated with nerve disability when compared with gunshot wounds, especially proximal to the elbow.<sup>5</sup> Blast wounds are a result of an extensive amount of energy transferred to the tissues involved. Acute imaging of combat wounds via DTI is not accurate because of the degree of inflammation and edema, which increases isotropy and results in artificial changes in diffusivities that do not reflect injury severity. In this study, we demonstrated that DTI tractography and ellipsoid mapping can overcome this challenge and can provide baseline nerve status following acute injury.

By applying voxel fiber orientation, we assessed the direction of movement of water molecules in the partial injured nerves, obtaining a better idea of these subtle changes in the axonal behavior. The dark blue areas in [Supplemental Figure 2](#) represent fiber orientation in *z*-axis correlated with healthy axonal behavior. These areas are seen proximally and distally to the injury, meaning that there is a large portion of the nerve caudally that is not harmed equally as proximal to the laceration. In other areas represented with polychromatic tones, values around the injury could correlate with isotropic movement of water molecules, meaning fiber orientation is dominant in the *x*- and *y*-axes. By quantifying the injured region and comparing it with the full axonal area, we were able to quantify the injury depth.

For SFI measurements, a score of less than  $-100$  translates to gait impairment, whereas closer to zero is considered normal behavior.<sup>17</sup> Poor scoring is determined by the fact that the distal toe spread is affected compared with the contralateral hind limb. This is controlled by the most distal muscle group of the extremity, requiring the most time to become reinnervated.<sup>17</sup> Previous animal models have been exhaustively studied on how motor dysfunction takes effect with a decrease in axonal population of more than 80%.<sup>6,7,18</sup> Clinical evaluations of our animals demonstrated that the degree of injury was comparable with their performance. In our study, we noticed that the worst clinical performance was correlated with the 75% injury at postoperative day 3 and with some recovery in the first week after surgery. This phenomenon was more noticeable with FF than in the SFI. Ganguly et al.<sup>17</sup> showed in their study how Sprague-Dawley rats treated with crush and with complete transection performed poorly at postoperative days 3 and 7, in which the crush group only started to recover only after almost day 10 after the intervention. Our rats recovered quicker because of the fact that only a portion of the nerve was affected, and the remaining untouched axons compensated, preventing poor scoring. We also noticed worse clinical performance in the first evaluation of the remaining groups, but in the 25% group, this decline was very subtle and returning to near baseline in

the subsequent evaluation of FF as well. In the half-injured cohort, the performance was in between the extreme groups, correlating with the degree of injury. Although previous work has shown associations between DTI parameters and clinical evaluations like leg contraction, rotarod treadmill (motor), and Von Frey filament, these previous experimental findings were after follow-ups of more than 1 week.<sup>19</sup>

Furthermore, when validating our DTT data with behavioral testing, these findings correlate accordingly with the amount of axonal damage. Even though our comparison is qualitative, we were able to pair the degree of injury with gait performance. Previous evaluation of early time points by quantitative DTI has been challenged, prompting the development of new tools, such as ellipsoid mapping to distinguish the varying degrees of injury. We also had the virtue to validate the accuracy of our novel device that we designed to reproduce the percentage of neurite injury. This prototype allows us to reproduce a partial nerve injury in an easy and consistent matter.

Previous animal studies have shown correlation between poor SFI scores and lower axon counts.<sup>20</sup> When obtaining histological parameters, total axon counts were performed. The amount of viable myelinated axons correlated linearly with the degree of injury produced to the nerve, in other words, the depth of the groove of the device manufactured in tridimensional plastic printing was associated with the same amount of healthy axonal population. Kakegawa et al.<sup>20</sup> attributed the correlation between injury and axonal counts was mostly because of the size of myelinated axons, or possibly because small regenerating axons escape the resolution of light microscopy.<sup>20</sup> However, the number of distal axons does not always reflect the amount of cell bodies proximal to the injury possibly because of the axonal sprouting phenomenon. It has been demonstrated that motor axons can sprout into three new axons and sensory can sprout into six.<sup>6,21</sup> Perhaps performing retrograde labeling could determine the amount of cell bodies located proximal to the injury can be associated to the number of axons caudally to the injury.

The strength of this work is that our proposed technology can detect subtle changes in nerve architecture as early as 1 week. However, this is a murine model that will need to be established in larger animals, before translating to a human. In the past, Boyer et al.<sup>22</sup> attempted to study partial injuries of sciatic injuries with DTI. Unfortunately, they were unable to distinguish the percentage of laceration based on FA alone at that time and were unable to validate their results with histology.<sup>22</sup> Our group, in agreement with Takagi et al.<sup>19</sup>, observed that FA, RD, AD, and MD parameters are obscured by edema. For this reason, we focused our studies using semiquantitative tractography and diffusion directionality.

One of the limitations of this technology is that most soldiers have been injured by explosions that can have shrapnel making DTI impossible. However, with serial débridements,

these fragments could be excised before scanning, though this should be kept in consideration when applying this technology to monitor our wounded soldiers. Nevertheless, obtaining data as early as possible would be extremely beneficial to surgeons, in that they could predict which nerve repairs are going to succeed or fail and thereby determine if another intervention is required, defeating the lengthy race against muscle atrophy. In this study, our results were as early as 7 days, but considering that this was a controlled animal population with an isolated injury, when it comes to translate to humans; we still need to do more studies with complex wounds to be able to apply this technique to our wounded soldiers. The fact that we were able to validate our results this early makes us very optimistic in DTI as peripheral nerve injury monitoring device. The main strength of this technology is not in the acute setting, we believe that the benefits of this monitoring tool is more in the subacute phase, when all life-threatening injuries have subsided, and the remaining question is if nerve function will favor limb salvage or amputation. This was the main reason why we chose to do an isolated nerve injury, to avoid surrounding tissue bias when collecting our data. Using DTT to monitor peripheral nerve outgrowth makes sense because of that they represent fiber tracts that reflect axonal architecture.<sup>23</sup> DTT has proven that this representation can orientate surgeons to preoperatively design a surgical plan when resecting a benign or malignant tumor.<sup>23</sup> The main focus of our laboratory is to find an alternative that can help reintroduce our disabled warriors back in to a productive society or at least routine daily activities. Having premature information about the neurological status of the limb will aid in determining if a surgical intervention (redo neuroorrhaphy, conduit, or nerve transfer) is required to avoid irreversible muscular atrophy. Our results in rat sciatic nerves hold promise for the possible translation of these technologies into humans in vivo.<sup>19</sup>

Future studies include an in vivo protocol design allowing us to follow longitudinally, a single larger animal.<sup>11</sup> This will allow us to monitor the effects of inflammation and edema in real time and reduce the number of animals studied while minimize suffering. This will also eliminate the detrimental effect that fixation of the nerve has over isotropic diffusion.<sup>24</sup> Scanning the same subject will need a qualified team able to induce anesthesia and monitor vital signs, as well as a developed facility. This allocation must be conditioned to perform scans for long periods of time, minimizing motion that could distort the image captured.<sup>11,23</sup> Additionally, more advanced diffusion models that account for the presence of edema are being investigated.

## CONCLUSIONS

These results indicate that orientation information from high-resolution DTT of ex vivo may provide viable biomarkers of peripheral recovery in the presence of edema in a rat sciatic nerve injury model, even in cases where scalar indices are corrupted. These findings suggest that we can differentiate

injury severity via DTI ellipsoids without the necessity to wait for the edema to subside.

## SUPPLEMENTARY MATERIAL

Supplementary material is available at *MILMED* online.

## REFERENCES

1. Chambers JA, Hiles CL, Keene BP: Brachial plexus injury management in military casualties: who, what, when, why, and how. *J Mil Med* 2014; 179(6): 640–4.
2. Mathieu L, Bertani A, Gaillard C, et al: Surgical management of combat-related upper extremity injuries. *Chir Main* 2014; 33(3): 174–82.
3. Birch R, Misra P, Stewart MP, et al: Nerve injuries sustained during warfare part I—Epidemiology. *J Bone Joint Surg Br* 2012; 94(4): 523–8.
4. Cross JD, Ficke JR, Hsu JR, Masini BD, Wenke JC: Battlefield orthopaedic injuries cause the majority of long-term disabilities. *J Am Acad Orthop Surg* 2011; 19(Suppl 1): S1–7.
5. Rivera JC, Glebus GP, Cho MS: Disability following combat-sustained nerve injury of the upper limb. *Bone Joint J* 2014; 96-B(2): 254–8.
6. Wood MD, Kemp SW, Weber C, Borschel GH, Gordon T: Outcome measures of peripheral nerve regeneration. *Ann Anat* 2011; 193(4): 321–33.
7. Poppler LH, Schellhardt LM, Hunter DA, et al: Selective nerve root transection in the rat produces permanent, partial nerve injury models with variable levels of functional deficit. *Plast Reconstr Surg* 2017; 139(1): 94–103.
8. Moore AM, Wagner II, Fox IK: Principles of nerve repair in complex wounds of the upper extremity. *Semin Plast Surg* 2015; 29(1): 40–7.
9. Bassilios Habre S, Bond G, Jing XL, Kostopoulos E, Wallace RD, Konofaos P: The surgical management of nerve gaps: present and future. *Ann Plast Surg* 2018; 80(3): 252–61.
10. Gilliat RW: Electrodagnosis and electromyography in clinical practice. *Br Med J* 1962; 2(5312): 1073–9.
11. Andersson G, Orådd G, Sultan F, Novikov LN: In vivo diffusion tensor imaging, diffusion kurtosis imaging, and Tractography of a sciatic nerve injury model in rat at 9.4T. *Sci Rep* 2018; 8(1): .
12. Jeon T, Fung MM, Koch KM, Tan ET, Sneag DB: Peripheral nerve diffusion tensor imaging: overview, pitfalls, and future directions. *J Magn Reson Imaging* 2018; 47(5): 1171–89.
13. Song SK, Sun SW, Ju WK, Lin SJ, Cross AH, Neufeld AH: Diffusion tensor imaging detects and differentiates axon and myelin degeneration in mouse optic nerve after retinal ischemia. *Neuroimage* 2003; 20(3): 1714–22.
14. Nguyen L, Afshari A, Kelm ND, et al: Bridging the gap: engineered porcine-derived urinary bladder matrix conduits as a novel scaffold for peripheral nerve regeneration. *Ann Plast Surg* 2017; 78(6S Suppl 5): S328–34.
15. Veraart J, Sijbers J, Sunaert S, Leemans A, Jeurissen B: Weighted linear least squares estimation of diffusion MRI parameters: strengths, limitations, and pitfalls. *Neuroimage* 2013; 81: 335–46.
16. Ramasamy A, Masouros SD, Newell N, et al: In-vehicle extremity injuries from improvised explosive devices: current and future foci. *Philos Trans R Soc Lond B Biol Sci* 2011; 366(1562): 160–70.
17. Ganguly A, McEwen C, Troy EL, et al: Recovery of sensorimotor function following sciatic nerve injury across multiple rat strains. *J Neurosci Methods* 2017; 275: 25–32.
18. Isaacs J, Mallu S, Wo Y, Shah S: A rodent model of partial muscle re-innervation. *J Neurosci Methods* 2013; 219(1): 183–7.

19. Takagi T, Nakamura M, Yamada M, et al: Visualization of peripheral nerve degeneration and regeneration: monitoring with diffusion tensor tractography. *Neuroimage* 2009; 44(3): 884–92.
  20. Kakegawa A, Yokouchi K, Itsubo T, et al: Correlation between motor function and axonal morphology in neonatally sciatic nerve-injured rats. *Anat Sci Int* 2015; 90(2): 97–103.
  21. Gordon T, Borschel GH: The use of the rat as a model for studying peripheral nerve regeneration and sprouting after complete and partial nerve injuries. *Exp Neurol* 2017; 287(Pt 3): 331–47.
  22. Boyer RB, Kelm ND, Riley DC, et al: 4.7-T diffusion tensor imaging of acute traumatic peripheral nerve injury. *Neurosurg Focus* 2015;39(3):E9.
  23. Vargas MI, Viallon M, Nguyen D, Delavelle J, Becker M: Diffusion tensor imaging (DTI) and tractography of the brachial plexus: feasibility and initial experience in neoplastic conditions. *Neuroradiology* 2010; 52(3): 237–45.
  24. Miller KL, Stagg CJ, Douaud G, et al: Diffusion imaging of whole, post-mortem human brains on a clinical MRI scanner. *Neuroimage* 2011; 57(1): 167–81.
-